

OPEN ACCESS

**Repository of the Max Delbrück Center for Molecular Medicine (MDC)
in the Helmholtz Association**

<http://edoc.mdc-berlin.de/15518>

CD20-targeting immunotherapy promotes cellular senescence in B-cell lymphoma

Daebritz, J.H.M. and Yu, Y. and Milanovic, M. and Schoenlein, M. and Rosenfeldt, M.T. and Doerr, J.R. and Kaufmann, A.M. and Dorken, B. and Schmitt, C.A.

This is the final version of the accepted manuscript. The original article has been published in final edited form in:

Molecular Cancer Therapeutics
2016 MAY ; 15(5): 1074-1081
2016 APR 20 (originally published online)
doi: [10.1158/1535-7163.MCT-15-0627](https://doi.org/10.1158/1535-7163.MCT-15-0627)

Publisher:
© 2016 American Association for Cancer Research

CD20-targeting immunotherapy promotes cellular senescence in B-cell lymphoma

J. Henry M. Däbritz,^{1,2} Yong Yu,³ Maja Milanovic,² Martin Schönlein,² Mathias T. Rosenfeldt,⁴ Jan R. Dörr,² Andreas M. Kaufmann,⁵ Bernd Dörken,^{1,2,3,6} and Clemens A. Schmitt^{1,2,3,6}

¹Charité – University Medical Center, Medical Department of Hematology, Oncology and Tumor Immunology, Campus Virchow Clinic, Berlin, Germany

²Charité – University Medical Center, Molekulares Krebsforschungszentrum, Berlin, Germany

³Max-Delbrück-Center for Molecular Medicine in the Helmholtz Association, Berlin, Germany

⁴Julius Maximilians University Würzburg, Department of Pathology, Würzburg, Germany

⁵Charité – University Medical Center, Gynecological Tumor Immunology, Campus Benjamin Franklin, Berlin, Germany

⁶Deutsches Konsortium für Translationale Krebsforschung (German Cancer Consortium), Partner site Berlin, Germany

Running title: Anti-CD20-mediated lymphoma cell senescence

Key words: B-cell lymphoma, cellular senescence, immunotherapy, Rituximab

Corresponding author: Prof. Dr. med. Clemens A. Schmitt
Charité – University Medical Center
Medical Department of Hematology, Oncology and Tumor Immunology
Campus Virchow Clinic
Augustenburger Platz 1
13353 Berlin, Germany
e-mail: clemens.schmitt@charite.de
Tel: +49 30 450 559 896 Fax: +49 30 450 553 986

Main text word count: 2713

Abstract word count: 211

Number of figures: 4

Number of tables: 1

Number of references: 47

Abbreviations: ADCC, antibody-dependent cellular cytotoxicity; ADR, Adriamycin; BrdU, Bromodeoxyuridine; CL, cross-linker; CLL, chronic lymphocytic B-cell leukemia; DDR, DNA damage response; DLBCL, diffuse large B-cell lymphoma; EBV, Epstein-Barr virus; FBS, fetal bovine serum; FSC, forward scatter; GSEA, gene set enrichment analysis; IL, interleukin; MCP-1, membrane cofactor protein-1; NAC, N-acetylcysteine; PI, Propidium iodide; ROS, reactive oxygen species; RTX, Rituximab; SA- β -gal, senescence-associated β -galactosidase; SASP, senescence-associated secretory phenotype; sCD40L, soluble CD40 ligand; SNP, single nucleotide polymorphism; SSC, side scatter, t-PA, tissue-type plasminogen activator; ut, untreated; VCR, Vincristine.

This work was supported by a Charité student fellowship to J.H.M. Däbritz as well as research support from the German Cancer Consortium (a.k.a. DKTK) and the Deutsche Krebshilfe (grant no. 108789) to C.A. Schmitt. The authors declare no competing financial interests.

Abstract

The CD20-targeting monoclonal antibody Rituximab is an established component of immunochemotherapeutic regimens against B-cell lymphomas, where its co-administration with conventional anti-cancer agents has significantly improved long-term outcome. However, the cellular mechanisms by which Rituximab exerts its anti-lymphoma activity are only partially understood. We show here that Rituximab induces typical features of cellular senescence, a long-term growth arrest of viable cells with distinct biological properties, in established B-cell lymphoma cell lines as well as primary transformed B-cells. In addition, Rituximab-based immunotherapy sensitized lymphoma cells to senescence induction by the chemotherapeutic compound Adriamycin (a.k.a. Doxorubicin), and, to a lesser extent, by the antimicrotubule agent Vincristine. Anti-CD20 treatment further enhanced secretion of senescence-associated cytokines, and augmented the DNA damage response (DDR) signaling cascade triggered by Adriamycin. As the underlying pro-senescence mechanism, we found intracellular reactive oxygen species (ROS) levels to be elevated in response to Rituximab, and, in turn, the ROS scavenger N-acetylcysteine (NAC) to largely abrogate Rituximab-mediated senescence. Our results, further supported by gene set enrichment analyses in a clinical data set of chronic lymphocytic leukemia patient samples exposed to a Rituximab-containing treatment regimen, provide important mechanistic insights into the biological complexity of anti-CD20-evoked tumor responses, and unveil cellular senescence as a hitherto unrecognized effector principle of the antibody component in lymphoma immunochemotherapy.

Introduction

The modes of action by which the CD20-targeting antibody Rituximab (RTX) produces clinical benefits in aggressive and indolent lymphoma are complex and have not been fully elucidated (1-3). It is well established that CD20-bound RTX recruits host immune effector principles such as antibody-dependent cellular cytotoxicity (ADCC) and complement-mediated cytotoxicity *via* its Fc domain (4-7). Moreover, RTX has been shown to slow proliferation and to induce apoptosis when tested against lymphoma cell lines in short-term assays (8), thereby contributing to the anti-tumor activity of conventional chemotherapeutic agents (3,9,10). However, in contrast to a lysosome-mediated cell death pathway that is triggered by so called type II CD20 antibodies, more recent studies reported only limited lymphoma cell death by the type I antibody Rituximab (11). Interestingly, although the signaling cascades evoked by different CD20-targeting compounds vary and remain poorly understood, ROS generation has been implicated as an important mechanism of response in CD20-targeted cells in different experimental settings (5,6,12,13).

Cellular senescence is a stress-responsive and ROS-inducible terminal arrest program that imposes a barrier to oncogenic transformation in preneoplastic lesions (14-17), has been observed in tumor specimens obtained from cancer patients after neo-adjuvant chemotherapy (18), and improves long-term outcome after anti-cancer chemotherapy in preclinical lymphoma models, especially when apoptosis is no longer available (19,20). Besides a distinct senescence-associated morphology and an increased activity of β -galactosidase at an acidic pH (SA- β -gal) (21,22), senescent cells display a senescence-associated secretory phenotype (SASP), representing a plethora of secreted factors largely consisting of cytokines and chemokines participating in the crosstalk between tumor cells, the microenvironment and the host immune system (23-25). While immune cells have been implicated in the anti-lymphoma cytotoxic activity of Rituximab *via* ADCC and related mechanisms, the spectrum of anti-tumor activities and potential non-cell-autonomous effects of this central immunotherapeutic agent have not fully been elucidated. Specifically, we

tested here whether CD20-directed immunotherapy with Rituximab drives lymphoma cell senescence, possibly associated with a secretory phenotype (SASP), and augments chemotherapy-induced senescence when applied in combination regimens.

Methods

Cell lines and treatments

The neoplastic B-lymphoid cell lines EHEB (chronic lymphocytic B-cell leukemia [CLL]) and RC-K8 (diffuse large B-cell lymphoma [DLBCL]) were obtained from M. Hummel (Charité) and authenticated in April 2013 using a single nucleotide polymorphism (SNP)-based multiplex approach (Multiplexion) (26). SNP profiles matched known profiles, or were unique. The SD-1 B-lymphoblastoid cell line (derived from a patient with acute lymphoblastic leukemia) and new reference stocks (authenticated by short tandem repeat-based methods) of EHEB and RC-K8 were obtained from German Collection of Microorganisms and Cell Cultures in December 2013. No mycoplasma contamination was detected in our regular tests until October 2015. Cells were cultured for a maximum of four weeks after initial thawing in RPMI containing 10% fetal bovine serum (FBS) and penicillin/streptomycin (100 Units/ml) and treated with Adriamycin, Vincristine (ADR, VCR, both from Sigma, at doses as indicated), or a saturating concentration (20 µg/ml) of Rituximab (RTX, Roche). F(ab')₂ fragments of rabbit-anti-human IgG (Rockland) were added as cross-linker (CL) at 50 µg/ml one hour after RTX to mimic clustering of RTX-bound CD20 *via* Fc receptor-expressing cells *in vivo*, reportedly augmenting signal transduction after ligation of CD20 (8,27). N-acetyl-cysteine (NAC, 2 mM, Hexal) was applied one hour prior to RTX or ADR in some experiments (5). In combined immunochemotherapeutic approaches, ADR or VCR were added four hours after CL. Compound administration, except for ADR and VCR, was repeated after three days, when cultures were subjected to a regular medium exchange. Cell culture supernatant was collected for cytokine analyses after overnight incubation of 10⁶ viable cells/ml in fresh media without FBS.

Generation of EBV-transformed B-lymphoid cells

Primary human B-cells were obtained from healthy volunteers after informed consent and approval by the local ethics committee of the Charité - Universitätsmedizin Berlin (EA

4/070/11), and infected with Epstein-Barr virus (EBV) supernatants derived from dense cultures of B95/8 cells as published (28). Continuously growing cell lines were treated with ADR, RTX and CL as described above.

Analysis of cell growth and SA- β -gal activity

Viability and cell density were assessed by trypan blue dye exclusion. Senescence-associated β -galactosidase (SA- β -gal) activity was detected as published (22), and quantified in more than five randomly selected areas (of > 200 cells each) in cytopsin preparations derived from at least two biological replications of the respective cells. Representative photomicrographs were taken using a CKX41 microscope equipped with a XC30 camera (Olympus).

Flow cytometry, cell-cycle profiling detection of cytokines and intracellular reactive oxygen species

Flow cytometric detection of forward and side scatter characteristics as well as CD20 expression (Beckman Coulter, IM 1451) was conducted on a Becton Dickinson FACS Calibur using BD Biosciences CellQuest Pro (version 4.02) and WinMDI (version 2.9) software. Cell-cycle distribution (Propidium iodide [PI] staining) combined with incorporation of bromodeoxyuridine (BrdU) were assessed as previously described (16). Cytokine concentrations were quantified using the FlowCytomix human cardiovascular kit (Bender MedSystems; BMS811FF) and FlowCytomix Pro software (version 2.2). Intracellular ROS levels were visualized with carboxy-2',7'-dichlorodihydrofluorescein diacetate (carboxy-H2DCFDA, 20 μ M; Invitrogen) following instructions of the manufacturer.

Protein expression analysis by immunoblotting

Immunoblotting of whole-cell extracts was performed as described previously (29), using primary antibodies for p53 (Santa Cruz Biotechnology, sc-126, 1:500 dilution), p53-P-Ser15 (Cell Signaling Technology, 9284, 1:1000), p21^{CIP1} (Santa Cruz Biotechnology, sc-397, 1:200), γ -H2AX (Cell Signaling Technology, 9718, 1:1000), H3K9me3 (Abcam, ab8898, 1:1000) and α -Tubulin (Sigma-Aldrich, T6199, 1:2000) as a loading control, with horseradish peroxidase-conjugated secondary antibodies (GE Healthcare, NA934V and NXA931).

Quantitative transcript and gene set enrichment analyses

Quantitative real-time reverse transcriptase PCR (RQ-PCR) for *interleukin (IL)-6* (Hs99999032_m1) and *IL-8* (Hs01567913_g1) mRNA expression were conducted after oligo-dT-primed cDNA synthesis for 45 cycles in a Step One Plus Real Time PCR system. Expression levels were calculated with *GAPDH* (Hs02758991_g1) as a housekeeping mRNA control as previously described (15). Gene Set Enrichment Analysis (GSEA), based on a publicly available data set generated from CD19⁺-selected peripheral blood CLL specimens and downloaded from the Gene Expression Omnibus web site (GEO; <http://www.ncbi.nlm.nih.gov/geo/query/acc.cgi?acc=GSE15490>), was performed with GSEA software (Version 2.0, Broad Institute, <http://www.broad.mit.edu/gsea>) (30,31). Gene sets were taken without further change from the indicated publication (32) or assembled from hallmark publications ('Senescence-related genes', Table S1) (23,33-35).

Statistical analyses

Normalized enrichment scores reflect a statistically significant enrichment for P values < 0.05 and false discovery rate values < 0.25 (based on the non-parametrical Kolmogorov-Smirnov test). Experimental data were evaluated for statistical significance by employing the unpaired Student's t -test (two-tailed) using the Prism 5 for Windows (version 5.01) software package (GraphPad Software). "*" indicates statistical significance (with $P < 0.05$) in all figures.

Results and discussion

To determine the ability of RTX to induce cellular senescence, we analyzed the long-term responses of CD20-positive human B-cell lymphoma lines EHEB, RC-K8 and SD-1, which displayed typical features of cellular senescence following treatment with the DNA-damaging agent Adriamycin (ADR, Figure 1A,B), to RTX with and without addition of a cross-linking F(ab')₂ fragment (CL; hereafter referred to as RTX_{CL}). Unlike the growth kinetics observed in control settings, cell numbers remained virtually constant in ADR-treated samples, and increased much less upon single-agent exposure to RTX_{CL} (Figure 1A). Because RTX_{CL} treatment only modestly reduced cellular long-term viability (Figure S1), the RTX_{CL}-related marked suppression of cell growth cannot simply be explained by increased cell death. Importantly, senescence-reminiscent morphological and flow cytometric changes – enlarged cells with a vacuole-rich cytoplasm resulting in increased forward/side scatter values (15,18,36) – became detectable in substantial proportions of the cells following ADR or RTX_{CL} treatment, and corresponded to significantly increased fractions of SA-β-gal-positive cells in comparison to untreated controls (Figure 1B,C), with single-agent RTX_{CL} treatment being less efficient regarding its potential to induce senescence when compared to the chemotherapeutic agent at its given dose (Figure 1A-C). Hence, we provide here first-time evidence, based on a variety of parameters, that RTX treatment evokes a senescent phenotype in lymphoma cells. Consistent with this, a substantial reduction of DNA synthesis (*i.e.* BrdU-positive S-phase of the cell-cycle) could be detected in EHEB cells, in which the majority of cells displayed features of senescence after RTX_{CL} treatment ($P < 0.0001$). In line with previous characterizations of senescent cell populations, all cell lines exhibited a significant accumulation of cells in BrdU-negative S-phase following RTX_{CL} exposure ($P = 0.0009$ for EHEB, $P = 0.0018$ for RC-K8, and $P < 0.0001$ for SD-1 cells; Figure 1D and Table S1) (37).

Since many anti-lymphoma treatment protocols, especially against aggressive B-cell lymphomas, contain RTX in a combined immunochemotherapy regimen with conventional

chemotherapeutic agents such as the topoisomerase poison ADR or the antimicrotubule agent Vincristine (VCR) (1), another component of the CHOP regimen, we next analyzed the effects of an ADR/RTX_{CL} combination treatment on RC-K8 and SD-1 cells. Addition of RTX_{CL} led to a significant increase of the relatively low fractions of senescent cells that were detectable in response to a reduced dose of ADR (5 ng/ml in RC-K8, hereafter referred to as “ADR 5”, and 2 ng/ml in SD-1 [“ADR 2”], *i.e.* about half of the initial dose applied; Figure 2A, *cf.* to Figure 1). Accordingly, S-phase-reflecting DNA synthesis, analyzed in viable cells only, was profoundly decreased in two-compound-exposed RC-K8 and SD-1 cells when compared to single-agent treatments ($P < 0.0001$ for RC-K8, and $P = 0.0117$ for SD-1 cells; Figure 2B and Table S1). Moreover, fractions of cells in BrdU-negative S-phase, as documented before for RTX_{CL} single-agent settings (*cf.* Figure 1D), were, paralleling the increase of SA- β -gal-positive cells, significantly expanded ($P = 0.0001$ for RC-K8, and $P < 0.0001$ for SD-1 cells). Of note, ADR treatment did not induce increased membrane expression of the RTX target CD20 (Figure S2A), thereby excluding enhanced antibody efficacy *via* elevated receptor quantities. Therefore, we hypothesized that the high fractions of senescent cells only achieved after co-exposure to both RTX_{CL} and ADR may be a result of antibody-mediated sensitization towards senescence induction by the DNA-damaging chemotherapeutic agent ADR.

Thus, we next addressed potential amplifier effects of the co-therapeutic schedule on senescence-related signaling programs, the secretory phenotype and the DNA damage response (DDR) cascade in RC-K8 cells. Consistent with the dose-dependent fractions of senescent cells generated in response to ADR, we also found interleukin (IL)-6 and IL-8, two major components of the SASP (23,25), at much higher concentrations in the culture supernatant of RC-K8 cells exposed to 10 ng/ml instead of 5 ng/ml of ADR (Figure 2C). Again, the addition of RTX_{CL} resulted in further, significant induction of IL-6 and IL-8 with ADR at both concentrations tested, while RTX_{CL} alone produced only marginal effects regarding the expression of these cytokines and their release (Figures 2C,D, and S2B).

As persistent activation of the DDR signaling cascade is often considered a prerequisite for induction and maintenance of cellular senescence as well as for the SASP (14,23,37,38), we analyzed critical DDR components at the time of manifest senescence (Figure 2E) in the DLBCL cells. While single-agent RTX_{CL} had little impact on DDR signaling, co-treatment with RTX_{CL} strongly enhanced the protein levels of the serine 139-phosphorylated histone variant H2A.X (a.k.a. γ -H2AX), a marker related to DNA strand breaks, even further when compared to ADR-only settings. Underscoring our hypothesis that RTX may exert its pro-senescent potential *via* sensitization to ADR-induced DDR signaling, we found the serine 15-phospho-activated tumor suppressor p53 (p53-P-S15) as another DDR signaling component, together with stabilization of total p53 protein and increased protein levels of the senescence-implicated cell-cycle regulator and transcriptional p53 target p21^{CIP1} to be induced in ADR-senescent, but even more in RTX_{CL}/ADR-co-treated cells. Consistent with a sustained and particularly active DDR cascade promoting senescence in response to the combined treatment, we detected trimethylated lysine 9 of histone H3 (H3K9me3), the transcriptionally repressive chromatin modification that has been mechanistically linked to the selective silencing of E2F-dependent S-phase genes in senescence (15,16,39), at particularly high levels in ADR-treated cells co-exposed to RTX_{CL} (Figure 2E). Of note, the microtubule-disrupting anti-lymphoma agent VCR, which does not primarily target DNA replication but induces p53 phosphorylation and interferes with DNA repair in cancer cells as well, also showed, like ADR, albeit less pronounced, significant collaborative senescence-inducing effects when RTX_{CL} was added (Figure 2F; *cf.* Figure 2A) (40,41). Taken together, Rituximab and conventional chemotherapy cooperatively induce senescence *via* sensitization to pro-senescent DDR signaling.

Elevation of intracellular ROS levels has been identified as a response to RTX in other settings (5,12), promotes DNA damage (29), and is a known trigger of cellular senescence as well (17,38). In line with this, we detected elevated ROS levels shortly after RTX_{CL} treatment (Figure 3A), and observed a complete loss of RTX-mediated senescence in the presence of the ROS scavenger N-acetylcysteine (NAC; Figure 3B,C; *cf.* Figure 1) in RC-K8

cells. Of note, NAC, at this dose, did not abrogate target cell binding of RTX (Figure S3A,B), and only moderately affected senescence entry in response to ADR (Figure 3C). These findings pinpoint ROS as the critical mediator of RTX-, but to a much lesser extent of ADR-induced senescence, thereby contrasting distinct RTX- vs. ADR-triggered senescence initiator pathways, which synergistically converge into p53-governed senescence effector signaling.

Although apoptosis- and senescence-regulating pathways are often defective in culture-adapted cancer cell lines (42), we were able to detect therapy-induced senescence after both ADR and RTX_{CL} in established lymphoma cell lines of B-cell origin. In order to validate our cell line model-based findings in primary human B-cells and primary human B-cell malignancies, we applied Rituximab to Epstein-Barr virus (EBV)-transformed, CD20-positive (data not shown) B-lymphoblastoid cells (28), and observed increased SA- β -gal reactivity in response to RTX_{CL} treatment as well as augmented senescence levels in comparison to single-agent ADR after combined immunochemotherapy (Figure 4A,B). Hence, the pro-senescent activity of RTX as a monotherapy and even further in a chemo-co-therapeutic setting can be demonstrated in primary, transformed human B-cells as well.

Finally, to estimate the clinical contribution of senescence as an effector mechanism of an RTX-containing chemotherapeutic regimen, we aimed at testing senescence-related gene sets in transcriptome data obtained from responding vs. non-responding patients diagnosed with B-cell chronic lymphocytic leukemia (B-CLL). Specifically, we analyzed gene sets that had previously been identified as “fingerprints” of (replicative) senescence in human cells (32), or were assembled as “senescence-related” from pivotal publications (23,33-35) (Table S2), regarding their potential enrichment in a sequential gene expression data set derived from B-CLL patients who had just received the first cycle of standard immunochemotherapy with the anti-CD20 antibody RTX, and the DNA-damaging conventional chemotherapeutic agents Fludarabine and Cyclophosphamide (30). Strikingly, the sample set obtained from subsequently responding patients (*i.e.* achieving partial or complete remissions after three months of treatment) displayed an enrichment in several

senescence-associated gene sets already one day after treatment, while no concordant enrichment was seen in non-responders (*i.e.* those patients presenting with stable or progressive disease at three months; Table 1). Taken together, these results underscore a beneficial role for Rituximab-induced senescence regarding the clinical outcome of patients with a CD20-positive B-cell malignancy.

In essence, the evidence presented here marks cellular senescence as an additional effector program by which RTX exerts its anti-lymphoma potential, and argues for a ROS-mediated mechanism as the underlying mode of RTX-mediated senescence induction. When co-administered with classic DNA-damaging drugs such as ADR, RTX sensitizes to chemotherapy-induced senescence and potentiates the extent of senescence-related chemokine and cytokine secretion (16,33,34). Moreover, SASP reinforces senescence, and may further add to treatment efficacy *via* modulation of RTX-engaged immune cell action (33,34). Possibly operating similarly, the epidermal growth factor receptor-blocking antibody Cetuximab reportedly sensitizes lung cancer cells to irradiation-induced senescence (while not producing senescence on its own) (43), and recently, increased SA- β -gal activity became detectable after application of Obinutuzumab, another CD20-directed antibody, in a cell line-based model of follicular lymphoma (44). Importantly, RTX-induced senescence does not seem to primarily damage DNA, as other non-genotoxic stimuli have been shown to produce cellular senescence (16,20,45). However, RTX-induced and ROS-promoted sensitization to a DDR that is mounted by conventional chemotherapeutic agents provides an explanation for the senescence-facilitating effect of this CD20-directed treatment, and may in part account for the clinical benefit of therapeutic regimens that include RTX. Moreover, since senescent tumor cells were shown to attract immune cells to the tumor site (24,46), immunochemotherapy-induced senescence with its strongly elevated SASP could even further improve immune clearance of lymphoma cells *in vivo*. Further molecular elucidation of the complex interplay between conventional anti-cancer agents, Rituximab and, alternatively, other CD20-directed compounds with respect to senescence induction will open the clinical

perspective of specifically engaging the senescence program to further improve therapeutic outcome of lymphoma patients.

Acknowledgements

The authors would like to thank members of the Schmitt lab for helpful discussions of the data and Katharina Pardon for excellent technical assistance.

References

1. Coiffier B, Lepage E, Briere J, Herbrecht R, Tilly H, Bouabdallah R, et al. CHOP chemotherapy plus rituximab compared with CHOP alone in elderly patients with diffuse large-B-cell lymphoma. *N Engl J Med* 2002;346:235-42.
2. Robak T, Dmoszynska A, Solal-Celigny P, Warzocha K, Loscertales J, Catalano J, et al. Rituximab plus fludarabine and cyclophosphamide prolongs progression-free survival compared with fludarabine and cyclophosphamide alone in previously treated chronic lymphocytic leukemia. *J Clin Oncol* 2010;28:1756-65.
3. Weiner GJ. Rituximab: mechanism of action. *Semin Hematol* 2010;47:115-23.
4. Beum PV, Lindorfer MA, Taylor RP. Within peripheral blood mononuclear cells, antibody-dependent cellular cytotoxicity of rituximab-opsonized Daudi cells is promoted by NK cells and inhibited by monocytes due to shaving. *J Immunol* 2008;181:2916-24.
5. Bellosillo B, Villamor N, Lopez-Guillermo A, Marce S, Esteve J, Campo E, et al. Complement-mediated cell death induced by rituximab in B-cell lymphoproliferative disorders is mediated in vitro by a caspase-independent mechanism involving the generation of reactive oxygen species. *Blood* 2001;98:2771-7.
6. Cragg MS, Glennie MJ. Antibody specificity controls in vivo effector mechanisms of anti-CD20 reagents. *Blood* 2004;103:2738-43.
7. de Haij S, Jansen JH, Boross P, Beurskens FJ, Bakema JE, Bos DL, et al. In vivo cytotoxicity of type I CD20 antibodies critically depends on Fc receptor ITAM signaling. *Cancer Res* 2010;70:3209-17.
8. Mathas S, Rickers A, Bommert K, Dorken B, Mapara MY. Anti-CD20- and B-cell receptor-mediated apoptosis: evidence for shared intracellular signaling pathways. *Cancer Res* 2000;60:7170-6.
9. Suzuki E, Umezawa K, Bonavida B. Rituximab inhibits the constitutively activated PI3K-Akt pathway in B-NHL cell lines: involvement in chemosensitization to drug-induced apoptosis. *Oncogene* 2007;26:6184-93.
10. Jazirehi AR, Huerta-Yepez S, Cheng G, Bonavida B. Rituximab (chimeric anti-CD20 monoclonal antibody) inhibits the constitutive nuclear factor- κ B signaling pathway in non-Hodgkin's lymphoma B-cell lines: role in sensitization to chemotherapeutic drug-induced apoptosis. *Cancer Res* 2005;65:264-76.
11. Ivanov A, Beers SA, Walshe CA, Honeychurch J, Alduaij W, Cox KL, et al. Monoclonal antibodies directed to CD20 and HLA-DR can elicit homotypic adhesion followed by lysosome-mediated cell death in human lymphoma and leukemia cells. *J Clin Invest* 2009;119:2143-59.
12. Jak M, van Bochove GG, van Lier RA, Eldering E, van Oers MH. CD40 stimulation sensitizes CLL cells to rituximab-induced cell death. *Leukemia* 2011;25:968-78.

13. Honeychurch J, Alduaij W, Azizyan M, Cheadle EJ, Pelicano H, Ivanov A, et al. Antibody-induced non-apoptotic cell death in human lymphoma and leukemia cells is mediated through a novel reactive oxygen species dependent pathway. *Blood* 2012;119:3523-33.
14. Bartkova J, Rezaei N, Liontos M, Karakaidos P, Kletsas D, Issaeva N, et al. Oncogene-induced senescence is part of the tumorigenesis barrier imposed by DNA damage checkpoints. *Nature* 2006;444:633-7.
15. Braig M, Lee S, Loddenkemper C, Rudolph C, Peters AH, Schlegelberger B, et al. Oncogene-induced senescence as an initial barrier in lymphoma development. *Nature* 2005;436:660-5.
16. Reimann M, Lee S, Loddenkemper C, Dorr JR, Tabor V, Aichele P, et al. Tumor Stroma-Derived TGF-beta Limits Myc-Driven Lymphomagenesis via Suv39h1-Dependent Senescence. *Cancer Cell* 2010;17:262-72.
17. Takahashi A, Ohtani N, Yamakoshi K, Iida S, Tahara H, Nakayama K, et al. Mitogenic signalling and the p16INK4a-Rb pathway cooperate to enforce irreversible cellular senescence. *Nat Cell Biol* 2006;8:1291-7.
18. te Poele RH, Okorokov AL, Jardine L, Cummings J, Joel SP. DNA damage is able to induce senescence in tumor cells in vitro and in vivo. *Cancer Res* 2002;62:1876-83.
19. Schmitt CA, Fridman JS, Yang M, Lee S, Baranov E, Hoffman RM, et al. A senescence program controlled by p53 and p16INK4a contributes to the outcome of cancer therapy. *Cell* 2002;109:335-46.
20. Dorr JR, Yu Y, Milanovic M, Beuster G, Zasada C, Dabritz JH, et al. Synthetic lethal metabolic targeting of cellular senescence in cancer therapy. *Nature* 2013;501:421-5.
21. Chang BD, Broude EV, Dokmanovic M, Zhu H, Ruth A, Xuan Y, et al. A senescence-like phenotype distinguishes tumor cells that undergo terminal proliferation arrest after exposure to anticancer agents. *Cancer Res* 1999;59:3761-7.
22. Dimri GP, Lee X, Basile G, Acosta M, Scott G, Roskelley C, et al. A biomarker that identifies senescent human cells in culture and in aging skin in vivo. *Proc Natl Acad Sci U S A* 1995;92:9363-7.
23. Coppe JP, Patil CK, Rodier F, Sun Y, Munoz DP, Goldstein J, et al. Senescence-associated secretory phenotypes reveal cell-nonautonomous functions of oncogenic RAS and the p53 tumor suppressor. *PLoS Biol* 2008;6:2853-68.
24. Xue W, Zender L, Miething C, Dickins RA, Hernando E, Krizhanovskiy V, et al. Senescence and tumour clearance is triggered by p53 restoration in murine liver carcinomas. *Nature* 2007;445:656-60.
25. Kuilman T, Peeper DS. Senescence-messaging secretome: SMS-ing cellular stress. *Nat Rev Cancer* 2009;9:81-94.
26. Castro F, Dirks WG, Fahrnich S, Hotz-Wagenblatt A, Pawlita M, Schmitt M. High-throughput SNP-based authentication of human cell lines. *Int J Cancer* 2013;132:308-14.
27. Shan D, Ledbetter JA, Press OW. Apoptosis of malignant human B cells by ligation of CD20 with monoclonal antibodies. *Blood* 1998;91:1644-52.
28. Hill AB, Lee SP, Haurum JS, Murray N, Yao QY, Rowe M, et al. Class I Major Histocompatibility Complex-restricted Cytotoxic T Lymphocytes Specific for Epstein-Barr Virus (EBV) Nuclear Antigens Fail to Lyse the EBV-transformed B Lymphoblastoid Cell Lines against Which They Were Raised. *J Exp Med* 1995;181:2221-8.

29. Reimann M, Loddenkemper C, Rudolph C, Schildhauer I, Teichmann B, Stein H, et al. The Myc-evoked DNA damage response accounts for treatment resistance in primary lymphomas in vivo. *Blood* 2007;110:2996-3004.
30. Shehata M, Demirtas D, Schnabl S, Hilgarth M, Hubmann R, Fonatsch C, et al. Sequential gene expression profiling during treatment for identification of predictive markers and novel therapeutic targets in chronic lymphocytic leukemia. *Leukemia* 2010;24:2122-7.
31. Subramanian A, Tamayo P, Mootha VK, Mukherjee S, Ebert BL, Gillette MA, et al. Gene set enrichment analysis: a knowledge-based approach for interpreting genome-wide expression profiles. *Proc Natl Acad Sci U S A* 2005;102:15545-50.
32. Zhang H, Pan KH, Cohen SN. Senescence-specific gene expression fingerprints reveal cell-type-dependent physical clustering of up-regulated chromosomal loci. *Proc Natl Acad Sci U S A* 2003;100:3251-6.
33. Acosta JC, O'Loghlen A, Banito A, Guijarro MV, Augert A, Raguz S, et al. Chemokine signaling via the CXCR2 receptor reinforces senescence. *Cell* 2008;133:1006-18.
34. Kuilman T, Michaloglou C, Vredeveld LC, Douma S, van Doorn R, Desmet CJ, et al. Oncogene-induced senescence relayed by an interleukin-dependent inflammatory network. *Cell* 2008;133:1019-31.
35. Wajapeyee N, Serra RW, Zhu X, Mahalingam M, Green MR. Oncogenic BRAF induces senescence and apoptosis through pathways mediated by the secreted protein IGFBP7. *Cell* 2008;132:363-74.
36. Chang BD, Xuan Y, Broude EV, Zhu H, Schott B, Fang J, et al. Role of p53 and p21waf1/cip1 in senescence-like terminal proliferation arrest induced in human tumor cells by chemotherapeutic drugs. *Oncogene* 1999;18:4808-18.
37. Di Micco R, Fumagalli M, Cicalese A, Piccinin S, Gasparini P, Luise C, et al. Oncogene-induced senescence is a DNA damage response triggered by DNA hyper-replication. *Nature* 2006;444:638-42.
38. Rodier F, Coppe JP, Patil CK, Hoeijmakers WA, Munoz DP, Raza SR, et al. Persistent DNA damage signalling triggers senescence-associated inflammatory cytokine secretion. *Nat Cell Biol* 2009;11:973-9.
39. Narita M, Nunez S, Heard E, Lin AW, Hearn SA, Spector DL, et al. Rb-mediated heterochromatin formation and silencing of E2F target genes during cellular senescence. *Cell* 2003;113:703-16.
40. Stewart ZA, Tang LJ, Pietenpol JA. Increased p53 phosphorylation after microtubule disruption is mediated in a microtubule inhibitor- and cell-specific manner. *Oncogene* 2001;20:113-24.
41. Poruchynsky MS, Komlodi-Pasztor E, Trostel S, Wilkerson J, Regairaz M, Pommier Y, et al. Microtubule-targeting agents augment the toxicity of DNA-damaging agents by disrupting intracellular trafficking of DNA repair proteins. *Proc Natl Acad Sci U S A* 2015;112:1571-6.
42. Drexler HG. Review of alterations of the cyclin-dependent kinase inhibitor INK4 family genes p15, p16, p18 and p19 in human leukemia-lymphoma cells. *Leukemia* 1998;12:845-59.
43. Wang M, Morsbach F, Sander D, Gheorghiu L, Nanda A, Benes C, et al. EGF receptor inhibition radiosensitizes NSCLC cells by inducing senescence in cells sustaining DNA double-strand breaks. *Cancer Res* 2011;71:6261-9.
44. Decaup E, Jean C, Laurent C, Gravelle P, Fruchon S, Capilla F, et al. Anti-tumor activity of obinutuzumab and rituximab in a follicular lymphoma 3D model. *Blood Cancer J* 2013;3:e131.

45. Wajapeyee N, Wang SZ, Serra RW, Solomon PD, Nagarajan A, Zhu X, et al. Senescence induction in human fibroblasts and hematopoietic progenitors by leukemogenic fusion proteins. *Blood* 2010;115:5057-60.
46. Kang TW, Yevsa T, Woller N, Hoenicke L, Wuestefeld T, Dauch D, et al. Senescence surveillance of pre-malignant hepatocytes limits liver cancer development. *Nature* 2011;479:547-51.
47. Coppe JP, Desprez PY, Krtolica A, Campisi J. The senescence-associated secretory phenotype: the dark side of tumor suppression. *Annu Rev Pathol* 2010;5:99-118.

Table 1. Predictive role of senescence-associated gene sets in patients diagnosed with chronic lymphocytic leukemia (CLL) undergoing RTX-based immunochemotherapy.

Gene signature	NR	R
Down in senescent fibroblasts	1.814	-1.769*
Up in senescent fibroblasts	-0.892	0.681
Down in senescent MEC	1.208	0.880
Up in senescent MEC	0.665	1.495*
Senescence-related genes	-0.893	1.514*

Tabular representation of nominal enrichment scores of gene sets comparing expression levels in tumor samples obtained 1 day post-treatment to specimens collected immediately before initiation of therapy in non-responding (NR, $n = 5$, left panel) and responding (R, $n = 5$, right panel) CLL patients undergoing immunochemotherapy with RTX, Fludarabine and Cyclophosphamide (30). “*” indicates significant (nominal P -value < 0.05) concordant regulation of the respective gene set. Gene sets reflect genes that had previously been found as up- or down-regulated in different senescent human cells (32), or were assembled as “senescence-related” in an unbiased fashion from pivotal publications (23,33-35).

Figure legends

Figure 1. Human lymphoma cells enter senescence in response to Rituximab-based immunotherapy. (A) Cell numbers of viable EHEB, RC-K8 and SD-1 cells at the indicated time-points relative to start of treatment with cross-linker (CL), Rituximab (RTX), combined RTX and CL (RTX_{CL}), Adriamycin (ADR; 10 ng/ml for EHEB and RC-K8, 5 ng/ml for SD-1), or left untreated (ut). Means of at least two independent experiments each performed in

triplicates are shown; arrow bars denote standard deviations. (B) Representative photomicrographs of cytospin preparations stained for senescence-associated- β -galactosidase (SA- β -gal) activity after six days. Scale bars indicated in controls correspond to 50 μ m (left panel) and 20 μ m (right upper panel) in all settings, numbers reflect mean percentages of SA- β -gal positive cells \pm standard deviations. Right lower panel: Flow cytometric analyses (density plots) of forward (FSC) and side (SSC) scatter characteristics of the corresponding cell populations after six days. (C) SA- β -gal activity in all scenarios tested. (D) Representative images of cell-cycle distribution as assessed by quantitative Propidium iodide (PI) staining (depicted on the X-axis) combined with incorporation of bromodeoxyuridine (BrdU, y-axis) 6 days after treatment as indicated. “**” denotes statistical significance of differences ($P < 0.05$) in (C) and (D).

Figure 2. Rituximab treatment augments chemotherapy-induced senescence via enhanced DNA damage signaling. (A) Representative SA- β -gal stainings, quantifications of SA- β -gal activity (generated in more than five randomly selected areas of > 200 cells each derived from at least two biological replications) and FSC/SSC density plots of RC-K8 and SD-1 cells six days after start of treatment (as in Figure 1B) with ADR concentrations that were incapable of inducing maximum senescence levels (5 ng/ml in RC-K8 cells [“ADR 5”] and 2 ng/ml in SD-1 [“ADR 2”]) as single agent or combined with RTX_{CL}. See Figure 1 for corresponding controls. (B) Comparison of BrdU/PI profiles of cells treated as in (A). (C) Representative flow cytometric multiplex bead-based fluorescence profiles of the indicated peptides in cell culture supernatants collected overnight from RC-K8 cells that had been treated as indicated for six days. Cytokine concentrations are plotted on the x-axis (logarithmic scale, log); bead populations corresponding to individual peptides are discriminated *via* peptide-specific fluorescence levels on the y-axis. Vertical marks indicate the positions of bead clouds corresponding to two major SASP cytokines, *i.e.* interleukin (IL)-6 (red) and IL-8 (blue) compared to untreated controls (hatched lines) for different ADR concentrations without RTX_{CL} (upper panel) or with RTX_{CL} (lower panel). IL-6 and IL-8

concentrations are indicated in the lower right corner of each panel (pg/ml, mean values \pm standard deviations from two independent experiments, each conducted in triplicate). No profoundly increased concentrations were detected for two other SASP factors tested (47), the tissue-type plasminogen activator (t-PA) and the membrane cofactor protein-1 (MCP-1). The soluble CD40 ligand (sCD40L) has to our knowledge not been described as a component of the SASP (23). (D) Quantitative RT-PCR analyses of *IL-6* (left) and *IL-8* (right) mRNA expression levels relative to untreated controls in RC-K8 cells exposed to the indicated treatments for six days. Arrow bars indicate standard deviations of two independent experiments performed in triplicates. (E) Western blot analyses of the indicated (phospho-) proteins in RC-K8 cells exposed for six days to ADR (5 or 10 ng/ml) and/or RTX_{CL} or left untreated. α -Tubulin serves as loading control. (F) Fractions of SA- β -gal-positive cells by Vincristine only (black bars, 2.5 ng/ml for RC-K8 and 0.5 ng/ml for SD-1) and with additional RTX_{CL} exposure (grey bars) in RC-K8 and SD-1 cells.

Figure 3. Rituximab-mediated senescence depends on ROS signaling. (A) Intracellular ROS levels (logarithmic scale) by carboxy-2',7'-dichlorodihydrofluorescein diacetate (carboxy-H₂DCFDA)-based flow cytometry after RTX_{CL} as compared to the untreated (ut) condition. Time-points at which detected differences were most pronounced (1 day for EHEB and SD-1, 4 hours for RC-K8) are shown. (B) Growth characteristics, morphology and SA- β -gal activity of RTX_{CL}-treated RC-K8 cells (as in Figure 1B) after pre-incubation with the ROS scavenger NAC. Note the increased number of cells in the RTX_{CL} setting despite impaired growth of controls with NAC pre-treatment (cf. Figure 1A). Again, values derived from two experiments, each conducted in three replicates, are shown. (C) Comparison of SA- β -gal reactivity (values generated as described in figure 1) in RC-K8 cells exposed to RTX_{CL} or ADR (10 ng/ml) in the presence or absence of NAC.

Figure 4. RTX-induced senescence in primary human Epstein-Barr virus (EBV)-transformed B-lymphoblastoid cells. (A) Representative visualizations of SA- β -gal

detection and FSC/SSC plots in four individual EBV-transformed B-lymphoblastoid cell preparations after six days of treatments as indicated. Numbers reflect mean percentages of SA- β -gal positive cells \pm standard deviations; scale bars in the control correspond to 50 μ m (left panel) and 20 μ m (right upper panel) in all settings. (B) Comparison of senescence levels achieved by single-agent ADR treatment (5 ng/ml) and additional RTX_{CL} as in Figure 2A ($n = 4$).

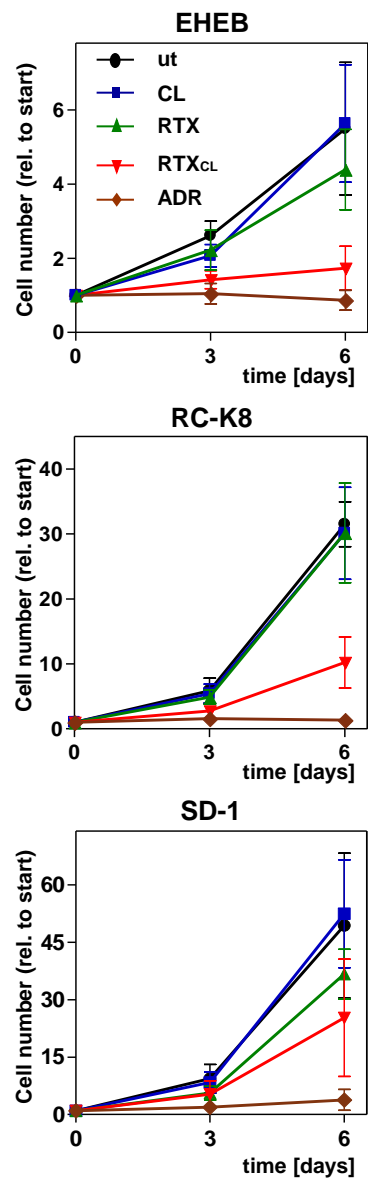
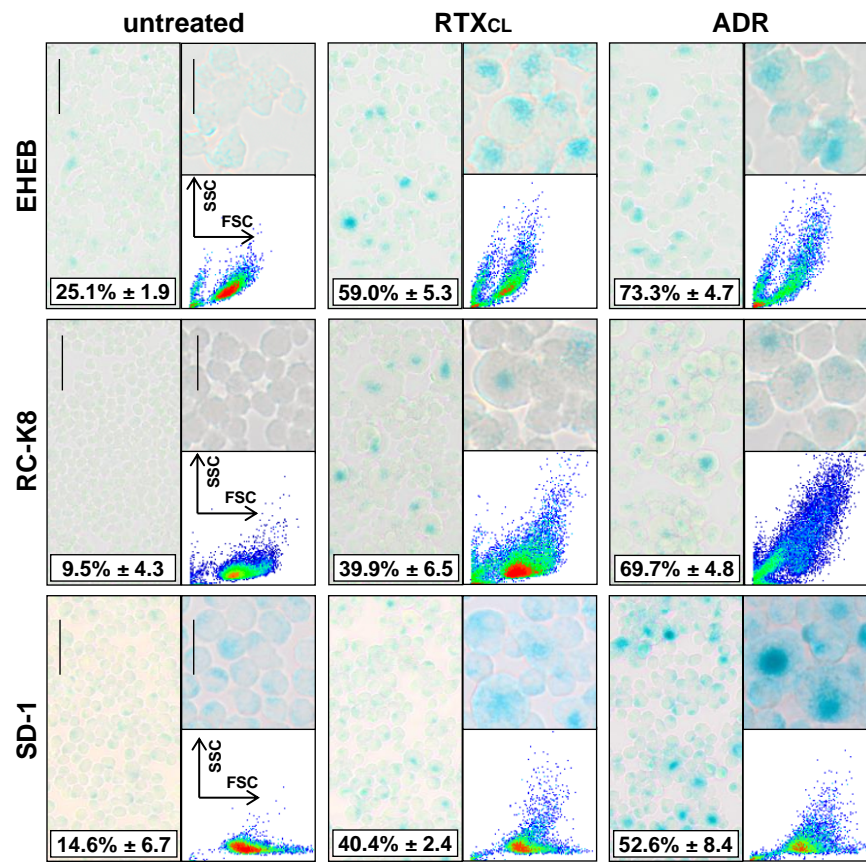
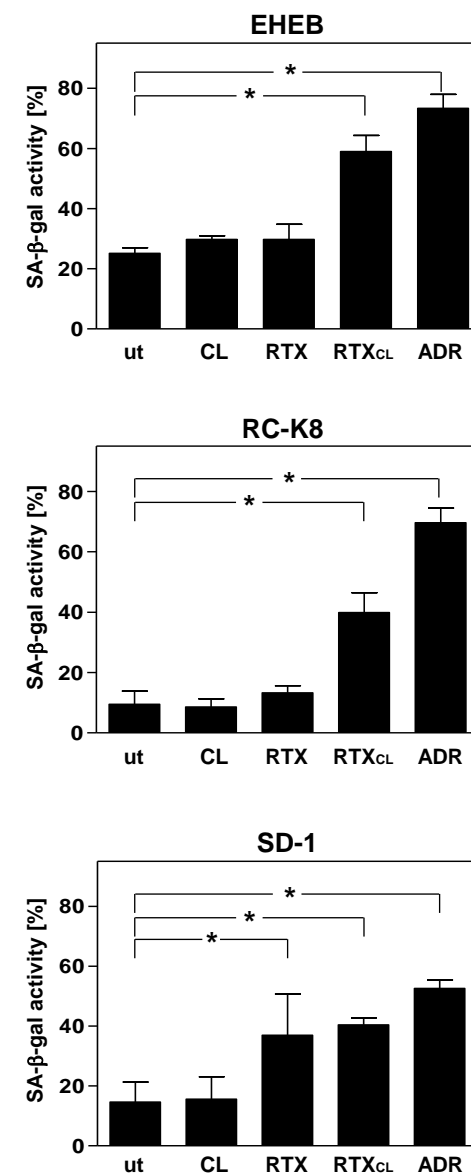
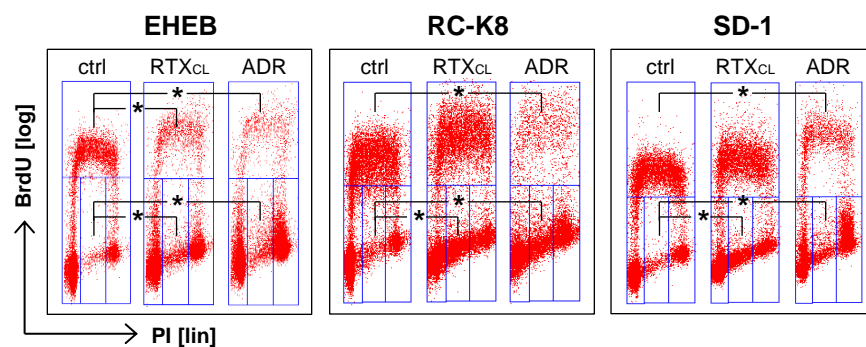
Fig. 1**A****B****C****D**

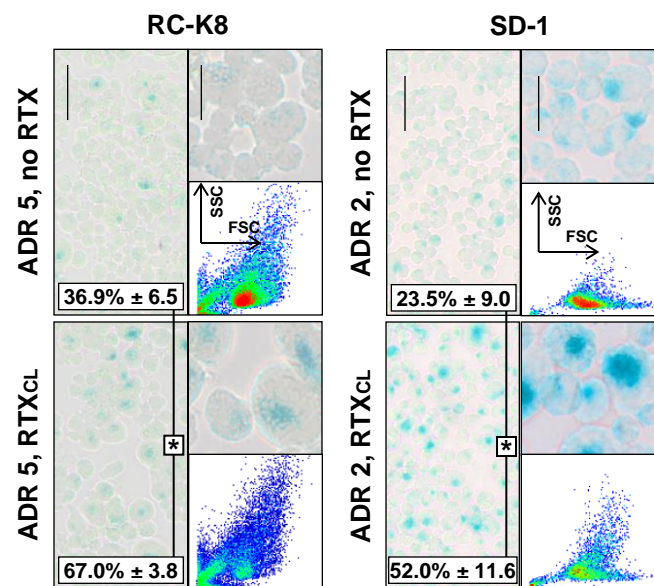
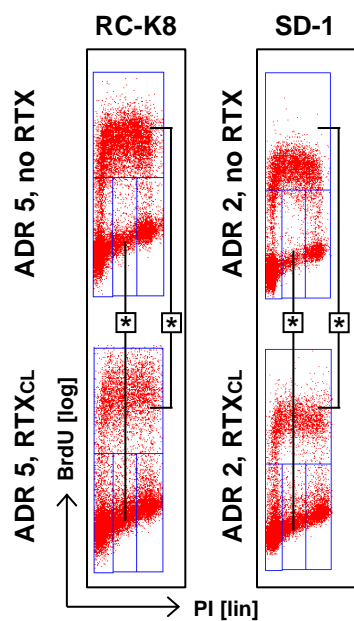
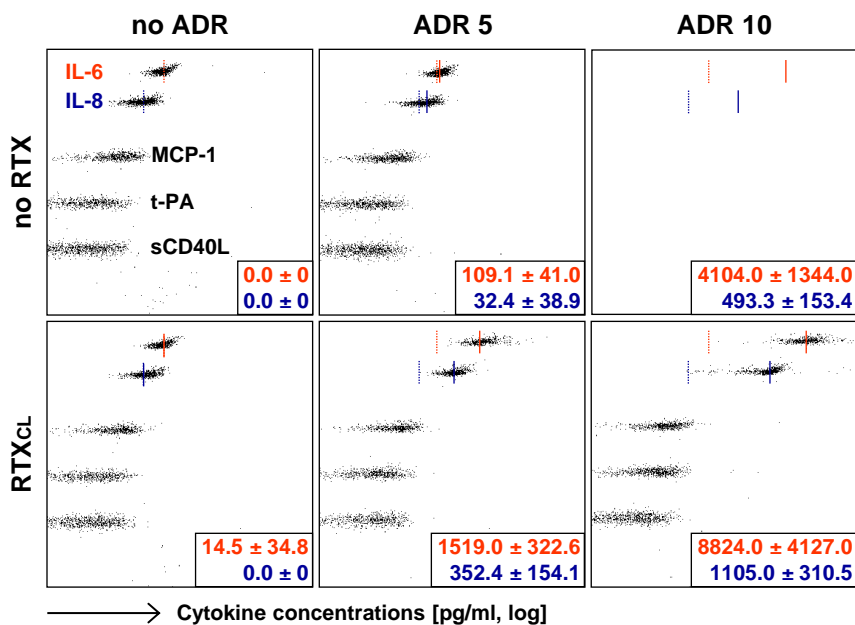
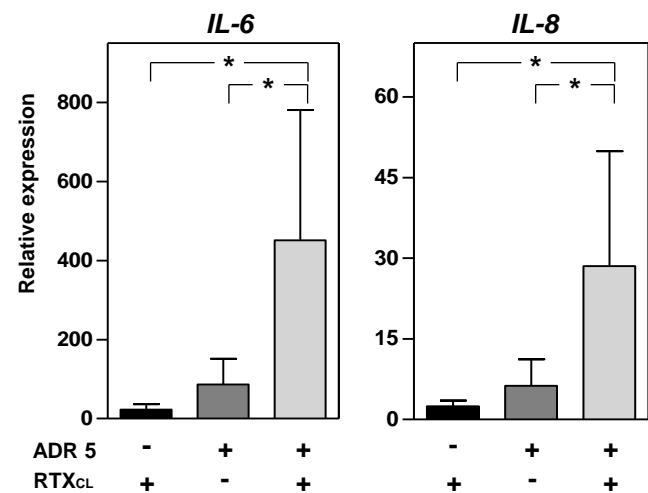
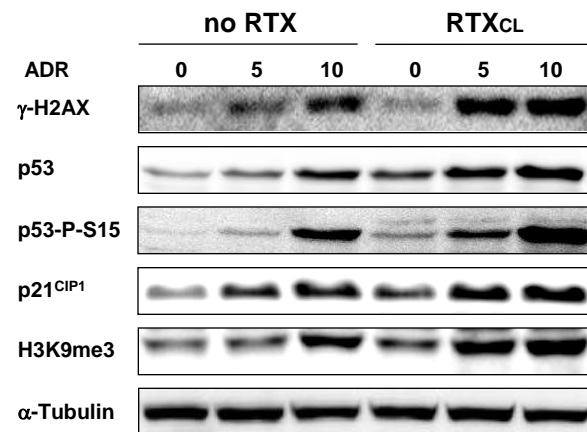
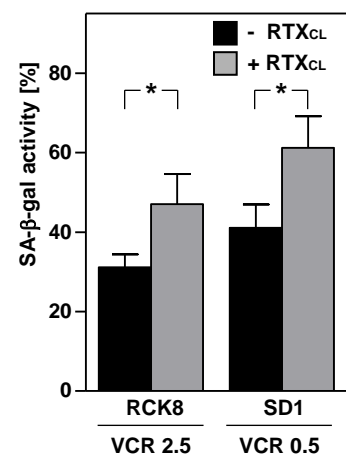
Fig. 2**A****B****C****D****E****F**

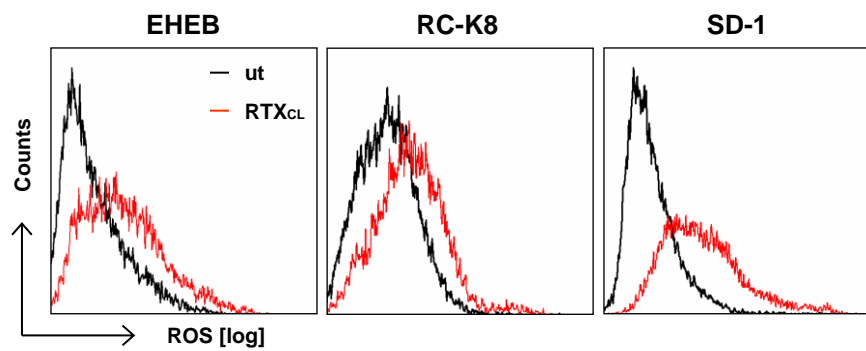
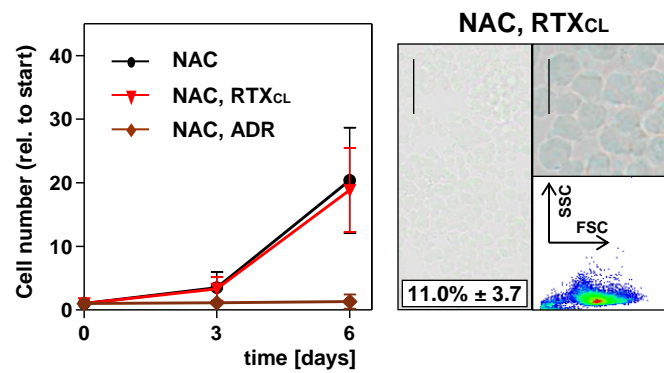
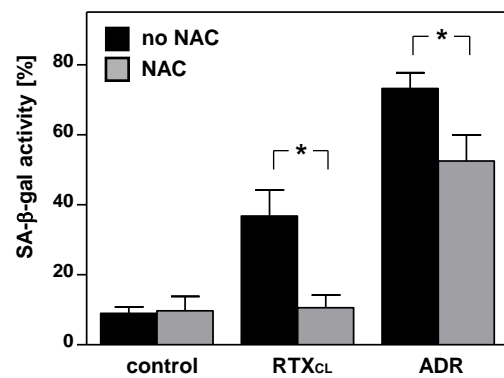
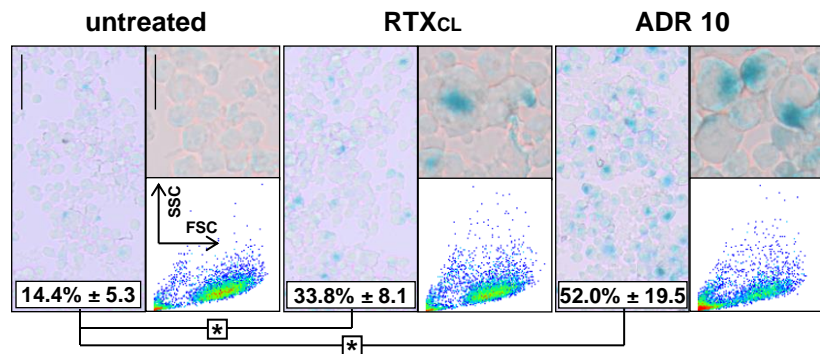
Fig. 3**A****B****C**

Fig. 4**A****B**